Astron. Astrophys. 357, 994–1000 (2000)

ASTRONOMY AND ASTROPHYSICS

Large [O]/[CO] ratios in cold molecular clouds towards W 49N⋆

C. Vastel[1], **E. Caux**[1], **C. Ceccarelli**[2], **A. Castets**[3], **C. Gry**[4,5], **and J.P. Baluteau**[4]

[1] CESR CNRS-UPS, B.P. 4346, 31028 Toulouse cedex 04, France
[2] Laboratoire d'Astrophysique, Observatoire de Grenoble, B.P. 53, 38041 Grenoble cedex 09, France
[3] Observatoire de Bordeaux, 2 Rue de l'Observatoire, B.P. 89, 33270 Floirac, France
[4] Laboratoire d'Astronomie Spatiale, Traverse du siphon, 13004 Marseille, France
[5] ISO Data Center, ESA Astrophysics Division, Villafranca del Castillo, P.O. Box, 59727 Madrid, Spain

Received 23 July 1999 / Accepted 27 March 2000

Abstract. We present ISO-LWS high spectral resolution (R $\sim$ 10^4) observations of the [OI] 63 μm and 145 μm lines towards the high mass star formation region W49N. At 145 μm the observed spectrum shows an emission component only, while at 63 μm it shows both emission and absorption components. We performed an analysis of the observed spectra using measured profiles of the LWS Fabry-Pérot spectral responses.

We also present ^{12}CO and ^{13}CO J = 1 $\rightarrow$ 0 and J = 2 $\rightarrow$ 1 observations of the same line of sight and detected seven molecular clouds.

We interpret the observed [OI] 63 μm line absorption as due to the oxygen associated with both atomic hydrogen clouds and molecular clouds present on the line of sight. We found that HI clouds are responsible only for a fraction of this absorption and that at least 15 times more O than CO has to be present in the molecular clouds to reproduce the observed 63 μm absorption. This implies that the gaseous oxygen is almost totally in atomic form and that carbon is deficient by more than a factor six in these molecular clouds.

Key words: ISM: abundances – ISM: atoms, ions – ISM: clouds – ISM: individual objects: W49N – ISM: molecules

1. Introduction

Oxygen is the most abundant element after hydrogen and helium in the Universe. It is therefore of prime importance to know in which form oxygen is found in the different phases of the Interstellar Medium. In the gas phase, all models (see Lee et al. 1996 and references therein) predict that CO, O[1] and O_2 are the major oxygen bearing species in molecular clouds.

However, several observational studies have ruled out that molecular oxygen is a major reservoir (Pagani et al. 1993; Maréchal et al. 1997; Olofsson et al. 1998). On the other hand, recent observations of the [OI] 63 μm line in absorption towards three massive star formation regions, DR21, SgrB2 and NGC 6334 (Poglitsch et al. 1996; Baluteau et al. 1997; Kraemer et al. 1998), revealed large O column densities between the sources and us and suggested that most of the oxygen is in the atomic form. Furthermore, Caux et al. (1999) reported the detection of the [OI] 63 μm and 145 μm lines in emission towards the molecular cloud L1689N. The observed fluxes imply a large O column density, 50 times larger than the CO column density, as measured by previous millimeter line observations. Since both C and C+ do not seem to be major reservoirs of carbon in L1689N, we concluded that carbon is largely depleted in this cloud and that oxygen is mainly in the atomic form.

It is of paramount importance to understand whether L1689N represents just a peculiar case or other molecular clouds share the same high [O]/[CO] ratio. For this reason we started a project aimed to obtain the [O]/[CO] ratio towards several massive star formation regions. In this paper we present the results relative to the W49N region, one of the most luminous regions of active star formation in the Galaxy. Located at $\sim$ 11.4 kpc from the Sun (Gwinn et al. 1992; they derived a Sun galactocentric distance equal to 8.1 kpc), behind the Galactic Center, W49N generates a total bolometric luminosity of 10^7 $L_\odot$ (Ward-Tompson & Robson 1990). Several atomic and molecular clouds are present along the W49N line of sight, which crosses twice the Sagittarius spiral arm (Nyman 1983). *These clouds, which absorb the high 63 μm continuum of W49N, are the target of our study.*

In this paper we report high resolution observations of the O line in absorption at 63 μm from which we derive the O column density, and CO observations from which we derive the CO column density. Sect. 2 presents the observations of the [OI] 63 μm and 145 μm lines, and of the ^{12}CO and ^{13}CO J = 1 $\rightarrow$ 0 and J = 2 $\rightarrow$ 1 lines. Sect. 3 presents the derivation of the column densities of O and CO. In Sect. 4 are the results discussed.

Send offprint requests to: C. Vastel (Charlotte.Vastel@cesr.fr)

⋆ Based on observations with ISO, an ESA project with instruments funded by ESA Member States (especially the PI countries: France, Germany, the Netherlands and the United Kingdom) with the participation of ISAS and NASA.

[1] In this paper we use the following nomenclature: O refers to the atomic oxygen as a chemical species; [O] to indicate the atomic oxygen abundance; and [OI] 63 μm and 145 μm to indicate the fordidden lines of the atomic oxygen

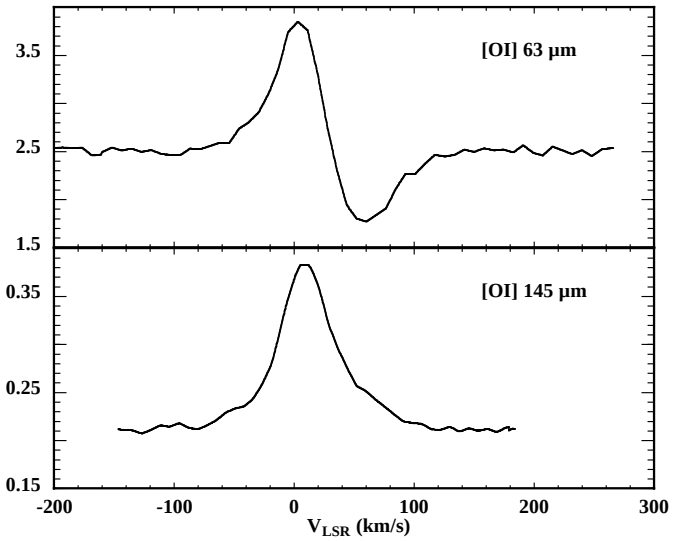

Fig. 1a and b. ISO-LWS high resolution spectra obtained towards W49N. **a** [OI] 63 μm, **b** [OI] 145 μm. Units are 10^{-8} ergs s^{-1} cm^{-2} μm^{-1}. The "grass" seen at the end of the spectra is the typical observational noise.

2. Observations and results

2.1. OI observations

2.1.1. Observations and data reduction

We performed high spectral resolution Fabry-Pérot (FP) observations centered on the [OI] 63 μm and 145 μm lines, using the Long Wavelength Spectrometer instrument (hereafter LWS: Clegg et al. 1996) on the ISO satellite (Kessler et al. 1996) using the L04 AOT. These observations, obtained during revolution 513, consisted of six scans per line, sampled at 1/4 of the FP resolution element. The total integration time on each sampling point was 2.4 sec. The $\sim 80''$ ISO-LWS beam was centered on the W49N coordinates ($\alpha_{2000} = 19^h\ 10^m\ 14^s.06$, $\delta_{2000} = 9^\circ\ 06'\ 22.3''$). The data were processed using the Off-Line-Processing pipeline version 7, and the latest improvements of the LIA (LWS Interactive Analysis version 7.3). A final analysis was made using the latest version of the standard package ISAP (version 1.6). Each spectrum was carefully deglitched scan by scan. The continuum level of the FP data was calibrated against observations of the same line of sight with LWS in the grating mode (L01 during revolution 513). L01 spectra are flux calibrated using Uranus, and the absolute accuracy is estimated to be better than 30% (Swinyard et al. 1998). Fig. 1 presents the observed [OI] 63 μm and 145 μm line profiles.

While the 145 μm line shows only an emission component, the 63 μm line shows both emission and absorption components. Indeed this is what is expected in presence of foreground cold and tenuous gas, since the upper level energy of the 145 μm transition is 326 K and is therefore not populated. Most of the oxygen atoms in this gas are in the ground state, where they can absorb the 63 μm photons of the high continuum. In Fig. 1 the emission component has been centered at 8 km s^{-1}, i.e. coincident with the velocity of the HII region. Note that the absolute uncertainty of LWS wavelength calibration is around 15 km s^{-1} (LWS handbook, Gry et al., 2000) but the relative uncertainty is much lower (< 2.5 km s^{-1}), allowing a very accurate determination of the velocity separation of the emission and absorption components. As already stated in the Introduction, the target of the present study is the material in the clouds along the line of sight, or in other words, the material which absorbs the 63 μm line. In the following we will therefore focus our discussion on the absorption component only and we postpone the study of the emission component to a forthcoming paper.

2.1.2. Determination of the LWS-FP instrumental profile

To disentangle instrumental effects from real features, we have first determined the instrumental responses at 63 μm and 145 μm of the LWS-FP. We used many observations of the NGC 7023 reflection nebula, obtained during the LWS calibration routine. NGC 7023 is chosen because of its narrow lines (≤ 3 km s^{-1}) in the ^{12}CO, ^{13}CO and C^{18}O molecules (Fuente et al. 1993). Assuming that the [OI] lines originate in the same quiescent medium, the profiles of the 63 μm and 145 μm lines observed towards this source give the relevant LWS-FP instrumental profiles.

The calibration observations consist of 250 scans, obtained through 13 different revolutions (between 258 and 837). The scans of each revolution were averaged together following the same method used for the W49N lines. However, since at each revolution a different setting of the instrument was used, the line center varied within 15 km s^{-1} (the absolute uncertainty of the LWS-FP wavelength calibration). The spectra obtained at each revolution were therefore re-centered in wavelength before averaging them together. The resulting spectra are shown in Fig. 2. The equivalent FWHM obtained are 43.9 km s^{-1} and 39.2 km s^{-1} at 63 and 145 μm respectively, to be compared with the 36 km s^{-1} and 33 km s^{-1} predicted by the instrument optical model. This broadening is believed to partly result from transient effects in the LWS detectors that are not corrected in the pipeline[2]. It is known that the optical model probably does not exactly represent the instrument, therefore we used the NGC 7023 averaged line spectra as the instrumental responses.

2.2. CO observations

The analysis presented in this paragraph is based on observations of the ^{12}CO and ^{13}CO J = 1 $\rightarrow$ 0 and J = 2 $\rightarrow$ 1 lines made in May and November 1999 with the 15m SEST telescope (ESO - La Silla, Chile). We simultaneously used two SIS receivers at 115 and 230 GHz (each one feeded with a different polarization), connected to an Acousto-Optic Spectrometer that provided a spectral resolution of 43 kHz in the two bands (0.105 and 0.217 km s^{-1} respectively). Typical SSB system temperatures during the observations were 190–250 and 250–380 K in

[2] Note that all the scans in the FP mode are obtained increasing the mesh separation, which implies scanning the line always in the same velocity direction.

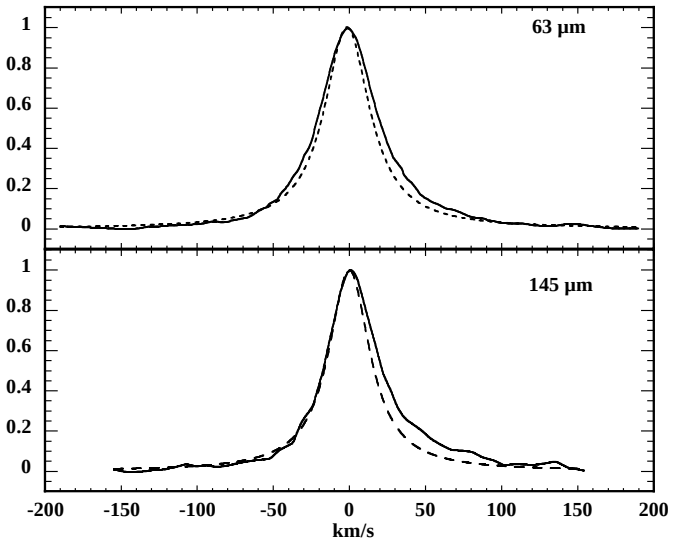

Fig. 2a and b. ISO-LWS FP's instrumental profiles (solid lines) obtained observing the reflection nebulae NGC 7023 compared with the theoretical ones (dashed lines). **a** [OI] 63 μm, **b** [OI] 145 μm.

Table 1. V_{LSR}, peak main beam temperature (T_{mb}) and FWHM of the CO lines averaged on the LWS beam for the seven velocity components in the line of sight of W49N. The FWHMs refer to ^{13}CO lines, when they are detected, or ^{12}CO lines, when ^{13}CO is not detected.

Cloud	V_{LSR}	^{12}CO (K)		^{13}CO (K)		FWHM
	km s^{-1}	(1-0)	(2-1)	(1-0)	(2-1)	km s^{-1}
abs1	34.7	1.30	0.30	<0.083	<0.118	1.9
abs2	40.8	3.71	3.08	1.19	0.52	1.7
abs3	53.5	0.43	0.24	<0.083	<0.118	1.9
abs4	56.0	0.90	0.76	<0.083	<0.118	1.7
abs5	61.0	1.24	1.20	0.26	0.14	2.2
abs6	64.7	2.61	2.50	0.93	0.67	1.6
abs7	70.5	0.29	0.38	<0.083	<0.118	1.9

the two bands respectively. The beam size is 45″ at 115 GHz and 23″ at 230 GHz. Pointing and focus were monitored regularly, and pointing corrections were always found smaller than $\sim 3''$. We performed a five point cross around the nominal position of the W49N HII region, with a 30″ spacing between the points. The goal was to obtain the emission line spectra averaged on the ISO-LWS beam in order to compare CO and O observations. The five spectra were therefore corrected for beam efficiency and convolved with a gaussian weighting function to degrade the resolution of the SEST beam to 80″, approximate size of the LWS beam at 63 μm, measured using Mars observations (LWS handbook, Gry et al., 2000). All temperatures quoted in this article are main beam temperatures.

Fig. 3 shows the ^{13}CO and ^{12}CO J = 1 $\rightarrow$ 0 and J = 2 $\rightarrow$ 1 line spectra at $V_{LSR} \geq 25$ km s^{-1}, where the [OI] 63 μm line is seen in absorption. The figure shows up to seven velocity components, whose parameters are reported in Table 1. These components correspond to seven molecular clouds in the line of sight. Three of these clouds are also detected in the ^{13}CO lines, implying optically thick ^{12}CO lines. The other four clouds are not visible in the ^{13}CO lines either because the ^{12}CO lines are optically thin or their emission extends less than the SEST beam.

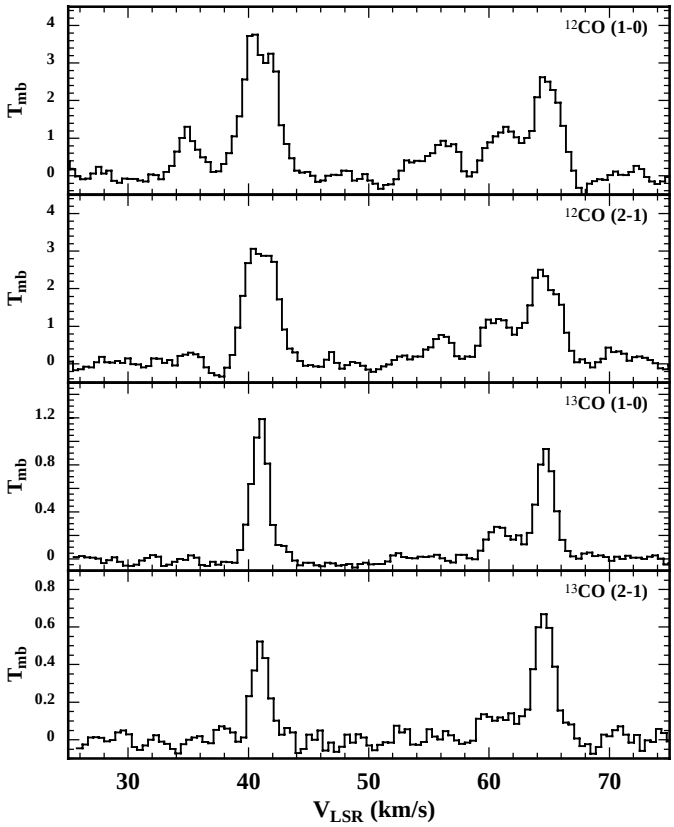

Fig. 3. ^{12}CO and ^{13}CO J = 1 $\rightarrow$ 0 and J = 2 $\rightarrow$ 1 line spectra degraded to the LWS beam (see text). Only velocities larger than 25 km s^{-1}, where the [OI] 63 μm line is observed in absorption, are shown. The velocity resolution is 0.4 km s^{-1}.

3. Column densities

This study is aimed at determining the [O]/[CO] ratio in the molecular clouds along the line of sight of W49N. The observations presented in the previous section permit to evaluate both the O and CO column densities. However, in our LWS observations of the [O] 63 μm line the spectral resolution is not enough to separate and identify the various components which may be responsible for the absorption of the 63 μm line. We know from our CO observations that there are seven molecular clouds which may absorb the 63 μm photons, *but* we also know that there are HI clouds along the line of sight as well. In order to estimate the [O]/[CO] ratio in the CO clouds we need to disentangle how much of the observed 63 μm absorption is due to the HI clouds and how much is due to the CO clouds themselves. In the following we first derive the HI and CO column densities respectively and then analyse the contribution of both HI and CO clouds to the 63 μm absorption.

3.1. HI

Previous observations of the 21 cm line by Lockhart & Goss (1978) were obtained with the Owens Valley Interferometer

with a spectral resolution of 0.84 km s^{-1}, in a beam ($\sim 2'$) comparable to the ISO-LWS one. Their Fig. 20b shows the HI line optical depth as a function of V_{LSR}. Assuming a spin temperature equal to 50 K, which is probably an upper limit to the true spin temperature in such clouds (see Eq. (1) in Liszt 1983), we derived for each cloud an upper limit to the HI column density using the standard relation:

$$N(HI) = 1.823 \times 10^{18} \times T_{spin} \times \int \tau(v) dv (cm^{-2}) \qquad (1)$$

The HI column densities derived for the four components at $V_{LSR} \geq 25$ km s^{-1} recognized by Lockhart & Goss (1978) are reported in Table 2. These atomic clouds could trace the photodissociation regions (PDR) in a shell around the main molecular clouds seen in CO.

3.2. CO

From our CO observations we derived the column densities of each of the seven molecular clouds listed in Table 1, using a standard LVG model described in Castets et al. (1990). In the three clouds where the ^{13}CO emission is detected (W49N-abs2, W49N-abs5 and W49N-abs6), we used both the ^{13}CO and ^{12}CO lines to *simultaneously* compute the density, temperature and CO column density (Table 3). In the remaining four clouds we assumed a gas temperature of 7 K (the average value from the three other clouds) and a density of 5×10^3 cm^{-3} (the typical value for a molecular cloud: note that a more accurate determination of the density is unnecessary in these computations as the lines are thermalized). Then we computed an upper limit to the CO column density in these four clouds using as an input to our LVG program a T_{mb} equal to 3 times the rms of our ^{13}CO observations (Table 1). The derived CO column densities for each component are reported in Table 3. Note that we used the isotopic ratio ^{12}C/^{13}C = 60 (Wannier 1980).

3.3. O

The derivation of the O column density from the 63 μm absorption is in principle straigthforward, once the linewidth of the absorbing region is known and assuming that in this region all oxygen atoms are in the ground state. In fact the optical depth at the line center is directly proportional to the atomic oxygen column density N(O) through the relation (Spitzer 1978):

$$\tau_0 = \frac{1.497 \times 10^{-2}}{b} \times N(O) \times \lambda \times f_{lu} \qquad (2)$$

where f_{lu} is the oscillator strength of the line defined as:

$$f_{lu} = 1.49919 \times \lambda^2 \frac{g_u}{g_l} A_{ul} \qquad (3)$$

g_u is the statistical weight of level u, $A_{ul} = 8.46 \times 10^{-5} s^{-1}$ is the Einstein coefficient of [OI] 63 μm transition (Baluja et al.1988), and b is the velocity spread parameter (b = FWHM/1.665), assuming a Maxwellian velocity distribution for the gas in the components. Thus, the column density of oxygen can be written:

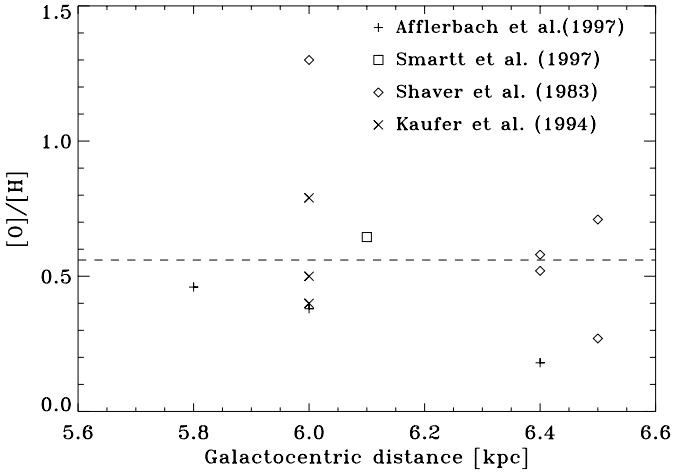

Fig. 4. Observations of the oxygen abundance as a function of the galactocentric distance between 5.6 and 6.6 kpc. References to the different symbols are reported in the upper right corner of the figure. The original points by Shaver et al. (1983) were rescaled here to account for the Sun galactic distance of 8.5 kpc. The dashed line represents the average oxygen abundance equal to 5.6×10^{-4}.

$$N(O) = 2.11 \times 10^{17} \times \tau_0 \times FWHM\ (cm^{-2}) \qquad (4)$$

where FWHM is the width of the absorbed atomic oxygen line.

We now compute separately the [O] 63 μm absorption due to the HI and CO clouds respectively.

a) [OI] 63 μm absorption from HI clouds.

In order to convert the HI column densities of Table 2 into O column densities, and compute then the 63 μm line absorption due to the HI clouds, the oxygen abundance in these clouds has to be known.

Several studies now show that the oxygen abundance is a function of the galactocentric distance (e.g. Afflerbach et al. 1997 and references therein). The clouds on the line of sight of W49 belong to the Sagittarius spiral arm at a galactic distance between 6 and 6.6 kpc (see Fig. 11 of Georgelin & Georgelin, 1976, with $l = 43.17°$ reported to $R_\odot$ = 8.5 kpc), compatible with their $V_{LSR} \geq 35$ km s^{-1} (see Fig. 19 of Burton 1991). In Fig. 4 we report all the observations of the oxygen abundance in the 5.6 to 6.6 kpc interval appeared in the literature (the relevant references are reported in the same figure). The average oxygen abundance obtained by these observations is 5.6×10^{-4}. This value is consistent with the study by Afflerbach et al. (1997), who found an oxygen abundance at 6 kpc equal to 5.8×10^{-4}, by measuring the oxygen abundance gradient in the Galaxy over a larger galactocentric distance interval.

To compute the N(HI) to N(O) conversion in the HI clouds along the W49N line of sigth, we adopted the average value of 5.6×10^{-4} and assumed that all oxygen is in the atomic form. The derived O column densities are reported in Table 2. From those O column densities we computed the opacity τ_o of the absorption lines following Eq. (4) (Table 2). Finally the 63 μm absorption due to the HI clouds obtained after convolution with

Table 2. Derived physical parameters and associated column densities of the four HI components identified towards W49N (see text).

V_{LSR} km s^{-1}	FWHM km s^{-1}	N(HI) 10^{21} cm^{-2}	N(O) 10^{18} cm^{-2}	τ_0(O)
35	10	2.4	1.4	0.6
40	5	1.1	0.6	0.6
59.8	17	4.9	2.7	0.8
63.5	12	1.5	0.8	0.3

Table 3. Computed temperature, density and CO and O column densities towards the seven molecular clouds in the line of sight (see Table 1).

Cloud	T K	n_{H_2} 10^3 cm^{-3}	N(^{12}CO) 10^{15} cm^{-2}	τ_0(O)	N(O) 10^{17} cm^{-2}
abs1	7	5	< 18	< 4.0	< 16.5
abs2	7	4.2	140	35.0	126.0
abs3	7	5	< 18	< 4.0	< 16.5
abs4	7	5	< 18	< 4.5	< 16.5
abs5	5	87	41	8.1	37.5
abs6	9	80	100	27.0	91.5
abs7	7	5	< 18	< 4.0	< 16.5

the instrumental profile is shown in Fig. 5. The figure clearly shows that the O associated with the HI clouds, although responsible for a fraction of the absorption, *cannot* entirely reproduce the observed 63 μm absorption. In order for the HI clouds to be totally responsible for the observed absorption an oxygen abundance equal to 1.3×10^{-3} is necessary. Although we cannot totally exclude it, Fig. 4 shows that this is a very unlike possibility at more than $\sim 3\sigma$. Furthermore, we remind that in theses computations we already used an upper limit for the HI column density (see Sect. 3.1), strengthening this conclusion.

b) [OI] 63 μm absorption from CO clouds.

We considered the oxygen absorption from the material in the seven molecular clouds *simultaneously* with the O absorption from material in the HI clouds. In this case we took a constant value for the [O]/[CO] ratio and varied this value to obtain the best fit to the observations. The [O]/[CO] obtained with this procedure is an average value on the seven clouds, but the procedure has the advantage to minimize the number of free parameters of the fit. Also in this case we convolved the absorption from the CO clouds with the instrumental profile, assuming a gaussian profile for the theoretical oxygen absorption, whose linewidths are reported in Table 3. In the procedure to obtain the best fit we also considered the emission component, whose profile is gaussian with a FWHM equal to that derived from the 145 μm line, namely 16 km s^{-1}. Changing this linewidth more than 5% would fail to reproduce the observed profile. The best fit is obtained for [O]/[CO] ~ 90 and is shown in Fig. 5. The oxygen column densities derived with this procedure are reported in Table 3. Since the [O]/[CO] obtained with this procedure is an average value, we cannot exclude that some of the seven CO clouds have the more canonical [O]/[CO] ~ 1 value, but this would imply a much higher [O]/[CO] for the remaining ones.

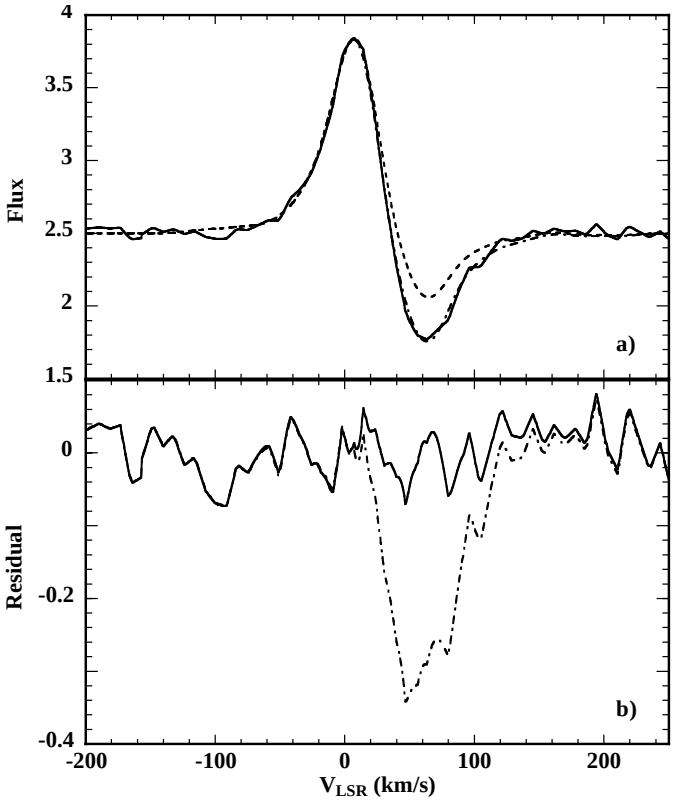

Fig. 5. a Comparison between the observed spectrum (full line), the derived spectrum for both CO and HI (dot-dashed line) and the computed spectrum for HI only (dashed line); **b** residuals between the observed spectrum and the constructed spectra: CO and HI (full line) and HI only (dot-dashed line); Units are 10^{-8} erg s^{-1} cm^{-2} μm^{-1}.

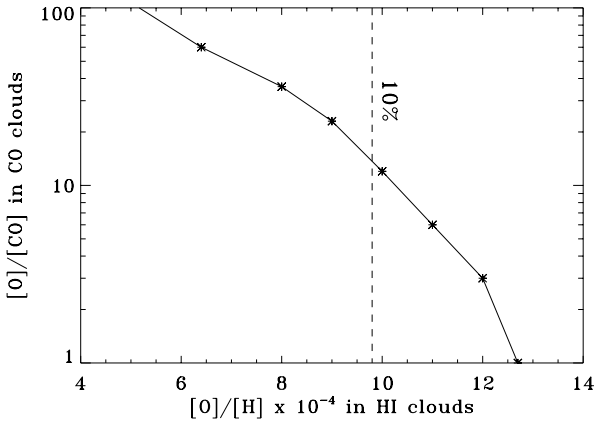

Fig. 6. The [O]/[CO] ratio in the CO clouds as a function of the oxygen abundance in the HI clouds.

Clearly, the [O]/[CO] ratio in the CO clouds critically depends on how much of the 63 μm absorption is due to the HI clouds, i.e. on the oxygen abundance in those clouds.

Fig. 6 shows this dependence, as derived by the procedure we described above. The dashed line in the figure marks the values of the oxygen abundance with a probability lower than 10%, i.e. 1.5σ times from the average derived in the previous paragraph (Fig. 4). The figure tell us that it is very unlikely

($\leq 10\%$) that [O]/[CO] ≤ 15 in average in the molecular clouds in the line of sight of W49N.

4. Discussion

In the previous section we showed that the observed 63 μm absorption is very unlikely to be totally attributable to the HI clouds along the line of sight, whereas at least half of it is very probably due to the CO clouds. The average O column density is $\sim 5 \times 10^{18}$ cm^{-2} in the clouds detected in the ^{13}CO and five times lower in the remaining ones. In these clouds the ratio [O]/[CO] is equal to 90, if the average value of the oxygen abundance (5.6×10^{-4}) applies to the HI clouds. [O]/[CO] is equal to 15 if a value 1.5σ times larger than the average applies. This ratio has a rather large value and certainly larger than the canonical [O]/[CO] ~ 1 value predicted by chemical models (e.g. Lee et al. 1996). This implies that very likely the almost totality of gaseous oxygen is in the atomic form and not locked into CO in the molecular clouds towards W49N. Taking the oxygen abundance equal to the average value (5.6×10^{-4}) at 6 kpc galactocentric distance, gives a hydrogen column density between 2.9×10^{21} cm^{-2} and 2.3×10^{22} cm^{-2} in the molecular clouds. Assuming that the standard A_V/N(H)=5.3×10^{-22} cm^{-2} applies, we obtain that the clouds along the line of sight have A_V between 1 and 12 mag. Note that *this is the molecular component only*, as we already "cleaned up" the O column density from the atomic component, which includes the atomic skin of the cloud, or in other word the Photo Dissociation Region (PDR) associated with each molecular cloud, where carbon is in the CII and CI forms (Tielens & Hollenbach 1985). These clouds are therefore relatively small and cold.

In the molecular clouds towards W49N (or some of them) there is definitively a *deficit of CO with respect to atomic oxygen*. Since carbon cannot be in the C+ or C form, it follows that *carbon is largely deficient in these molecular clouds with respect to O*. Unfortunately, the carbon abundance gradient in the Galaxy is poorly known. If the carbon abundance at 6 kpc is similar to the cosmic abundance of 2.4×10^{-4} (Cardelli et al. 1996), then carbon is depleted by at least a factor six.

Given the low kinetic temperatures of these molecular clouds (Table 3), it is very likely that most of carbon is locked into the grain mantles as iced CO and/or CO_2. In fact the evaporation temperature of pure CO ice is ~ 20 K and higher for CO_2 (Tielens et al. 1991) so that in cold enough clouds CO and/or CO_2 remain sticked onto the mantles. In support of this thesis, Chiar et al. (1995) found that more than 40% of CO is iced in quiescent regions of the Taurus cloud, while iced CO_2 has been found to have an abundance comparable to the iced CO in the quiescent cloud towards Elias 16 (Whittet et al. 1998).

Finally, evidence is now mounting that in quiescent cold clouds CO is largely depleted: recent examples include the case of L1544 where a CO depletion larger than a factor ten was observed (Caselli et al. 1999), or the case of IC 5146 where a similar depletion was found towards the innermost regions (Kramer et al. 1999), not to mention the case of L1689N (Caux et al. 1999) discussed in the Introduction.

5. Conclusions

We reported ISO-LWS high resolution ($\sim 10^4$) observations of the 63 μm fine structure line of atomic oxygen towards W49N. The line is found in absorption against the high W49N continuum at velocities $V_{LSR} \geq 25$ km s^{-1}.

Dedicated ground based observations of the ^{12}CO and ^{13}CO J = 1 $\rightarrow$ 0 and J = 2 $\rightarrow$ 1 transitions are also reported. We detected seven molecular clouds along the line of sigth of W49N at $V_{LSR} \geq 25$ km s^{-1}.

Using previous observations of HI emission towards W49N we derived the H column density of the atomic gas along the line of sight. Combining measured oxygen abundances at the distance of the clouds in the line of sight, we derived the relevant oxygen abundance and computed the absorption due to the atomic gas. Our first conclusion is that *HI clouds absorb only a fraction of the observed 63 μm absorption*.

The remaining 63 μm absorption is due to intervening molecular clouds seen in the CO transitions. *The [O]/[CO] ratio in those molecular clouds has to be larger than 15 to account for the observed 63 μm absorption.*

This implies a *carbon deficiency larger than a factor 6* with respect to the cosmic abundance. We suggest that this is probably due to CO/CO_2 depletion into grain mantles, if the carbon abundance at 6 kpc is similar to the carbon cosmic abundance.

Acknowledgements. We are grateful to an anonymous referee, whose comments significantly improved the first version of the manuscript. We also thank Teije de Jong, Jurgen Stutzki, Jose Cernicharo and Francois Boulanger for helpful discussions. We acknowledge the dedication of the LWS team which made these observations possible.

References

Afflerbach A., Churchwell E., Werner M.W., 1997, ApJ 478, 190
Baluja K.L., Butler K., Le Bourlot J., Zeippen C.J., 1988, J. Phy. S. 49, 129
Baluteau J.P., Cox P., Cernicharo J., et al., 1997, A&A 322, L33
Burton W.B., 1991, In: Pfenniger D., Bartholdi P. (eds.) The Galactic Interstellar Medium. Saas-Fee Advanced Course 21, Springer-Verlag
Cardelli J.A., Meyer D.M., Jura M., Savage B.D., 1996, ApJ 467, 334
Caselli P., Walmsley C.M., Tafalla M., Dore L., Meyers P.C., 1999, ApJ 523, L165
Castets A., Duvert G., Dutrey A., et al., 1990, A&A 234, 469
Caux E., Ceccarelli C., Castets A., et al., 1999, A&A 347, L1
Clegg P.E., Ade P.A.R., Armand C., et al., 1996, A&A 315, L38
Chiar J.E., Adamson A.J., Kerr T.H.,, Whittet D.C.B., 1995, ApJ 455, 234
Fuente A., Martin-Pintado J., Cernicharo J., Bachiller R., 1993, A&A 276, 473
Georgelin Y.M., Georgelin Y.P., 1976, A&A 49, 57
Gry C., on behalf of the LWS Consortium, 2000, LWS handbook, in preparation
Gwinn C.R, Moran J.M., Reid M.J., 1992, ApJ 393, 149
Kaufer A., Szeifert Th., Krenzin R., et al., 1994, A&A 289, 740
Kessler M.F., Steinz J.A., Anderegg M.E., et al., 1996, A&A 315, L27
Kraemer K.E., Jackson J.M., Lane A.P., 1998, ApJ 503, 785

Kramer C., Alves J., Lada C., Lada E., et al., 1999, A&A 342, 257
Lee H.H., Bettens R.P.M.,, Herbst E., 1996, A&AS 119, 111
Liszt H.S., 1983, ApJ 275, 163
Lockhart I.A., Goss W.M., 1978, A&A 67, 355
Maréchal P., Pagani L., Langer W.D., Castets A., 1997, A&A 318, 252
Nyman L.A., 1983, A&A 120, 307
Olofsson G., Pagani L., Tauber J., et al, 1998, A&A 339, L81
Pagani L., Langer W.D., Castets A., 1993, A&A 274, L13
Poglitsch A., Herrmann F., Genzel R., et al., 1996, ApJ 462, L43
Shaver P.A., McGee R.X., Newton L.M., et al., 1983, MNRAS 204, 53
Smartt S.J., Rolleston W.R.J., 1997, ApJ 481, L47
Spitzer L., 1978, In: Physical Processes in the Interstellar Medium. John Wiley & Sons, p. 52
Swinyard B.M., Burgdorf M.J., Clegg P.E., et al., 1998, SPIE 3354, 888
Tielens A.G.G.M., Hollenbach D., 1985, ApJ 291, 722
Tielens A.G.G.M., Tokunaga A.T., Geballe T.R., Baas F., 1991, ApJ 381, 181
Wannier P.G., 1980, ARA&A 18, 399
Ward-Thompson D., Robson E., 1990, MNRAS 244, 458
Whittet D.C.B., Gerakines P.A., Tielens A.G.G.M., Adamson A.J., et al., 1998, ApJ 498, L159